Multimodality Intravascular Imaging to Predict Periprocedural Myocardial Infarction During Percutaneous Coronary Intervention

CrossMark

Annapoorna S. Kini, MD, Sadako Motoyama, MD, PhD, Yuliya Vengrenyuk, PhD, Jonathan E. Feig, MD, PhD, Jacobo Pena, MD, Usman Baber, MD, Arjun M. Bhat, MD, Pedro Moreno, MD, Jason C. Kovacic, MD, PhD, Jagat Narula, MD, PhD, Samin K. Sharma, MD

ABSTRACT

OBJECTIVES The aim of this study is to compare the relative merits of optical coherence tomography (OCT), intravascular ultrasound (IVUS), and near infrared spectroscopy (NIRS) in patients with coronary artery disease for the prediction of periprocedural myocardial infarction (MI).

BACKGROUND Although several individual intravascular imaging modalities have been employed to predict periprocedural MI, it is unclear which of the imaging tools would best allow prediction of this complication.

METHODS We retrospectively analyzed 110 patients who underwent OCT, IVUS, and NIRS. Periprocedural MI was defined as a post-procedural cardiac troponin I (cTnI) elevation above $3\times$ the upper limit of normal; analysis was also performed for cTnI $\geq 5\times$ the upper limit of normal.

RESULTS cTnI $\geq 3\times$ was observed in 10 patients (9%) and 8 patients had cTnI $\geq 5\times$. By OCT, minimum cap thickness was significantly lower (55 vs. 90 μm, p < 0.01), and the plaque burden by IVUS (84 $\pm$ 9% vs. 77 $\pm$ 8%, p < 0.01) and maximum 4-mm lipid core burden index by NIRS (556 vs. 339, p < 0.01) were greater in the cTnI $\geq 3\times$ group. Multivariate logistic regression analysis identified cap thickness as the only independent predictor for cTnI $\geq 3\times$ the upper limit of normal (odds ratio [OR]: 0.90, p = 0.02) or cTnI $\geq 5\times$ (OR: 0.91, p = 0.04). If OCT findings were excluded from the analysis, plaque burden (OR: 1.13, p = 0.045) and maximum 4-mm lipid core burden index (OR: 1.003, p = 0.037) emerged to be the independent predictors.

CONCLUSIONS OCT-based fibrous cap thickness is the most important predictor of periprocedural MI. In the absence of information about cap thickness, NIRS lipid core or IVUS plaque burden best determined the likelihood of the periprocedural event. (J Am Coll Cardiol Intv 2015;8:937–45) © 2015 by the American College of Cardiology Foundation.

Myocardial damage after percutaneous coronary intervention (PCI) defined as cardiac troponin elevation has been reported as a procedural complication in about 10% to 50% of patients (1–4). Post-PCI cardiac troponin elevation has been reported to be associated with increased adverse short- and intermediate-term outcomes (5–10). This complication has been frequently attributed to large, lipid-rich plaques that could embolize and release necrotic debris into the distal circulation. Several intravascular imaging modalities such as optical coherence tomography (OCT) (11–14), intravascular ultrasound (IVUS) (3,14–16), IVUS–virtual histology (16), near infrared

ABBREVIATIONS AND ACRONYMS

CI = confidence interval

CSA = cross-sectional area

cTnI = cardiac troponin I

IVUS = intravascular ultrasound

LCBI = lipid core burden index

maxLCBI$_{4mm}$ = maximum 4-mm lipid core burden index

MI = myocardial infarction

MLA = minimal lumen area

NIRS = near infrared spectroscopy

OCT = optical coherence tomography

OR = odds ratio

PCI = percutaneous coronary intervention

TCFA = thin cap fibroatheroma

TIMI = Thrombolysis *in* Myocardial Infarction

ULN = upper limit of normal

spectroscopy (NIRS) (17,18), and noninvasive computed tomography angiography imaging (19,20) have been employed to predict periprocedural myocardial infarction (MI). Lesion characteristics, associated with this periprocedural complication, include a thin fibrous cap with wide lipid attenuation arc verified by OCT, large attenuated plaque area with positive remodeling detected by grayscale IVUS, large IVUS-virtual histology necrotic core, and virtual histology thin cap fibroatheroma (TCFA) (21), TCFA on radiofrequency IVUS, or high lipid core burden demonstrated by NIRS. All of these modalities have demonstrated variable effectiveness in predicting complications based on the strength of the employed imaging strategy. Although OCT, IVUS, and NIRS are all able to recognize lipid-rich plaques, it is still unclear which of these available imaging tools would allow for the most accurate prediction of periprocedural MI. Accordingly, we sought to simultaneously compare the IVUS, OCT, and NIRS imaging-based metrics for the risk of periprocedural MI in patients with stable ischemic heart disease.

METHODS

Study population. This study was a retrospective analysis of prospectively collected data from the institutional review board-approved clinical and multimodality imaging database. All procedures were done in the Mount Sinai Cardiac Catheterization Lab. The baseline demographic, clinical, procedural, and in-hospital outcomes data and imaging characteristics were obtained from the database. The study group comprised 133 consecutive patients referred for cardiac catheterization for evaluation of coronary artery disease who had undergone OCT and IVUS/NIRS imaging. All cases represented de novo atherosclerosis. Of these 133 patients, 23 were excluded because 18 patients had baseline cardiac troponin I (cTnI) levels above the upper limit of normal (ULN) and in 5 patients image quality was not deemed to be optimum. The remaining 110 patients were analyzed. One hundred and ten patients included in the study also formed a part of COLOR (Chemometric Observation of Lipid Core Plaques of Interest in Native Coronary Arteries) registry enrolled only from our center. Patients with renal failure (creatinine >1.5 mg/dl), hemodynamic compromise, contrast

allergy, and aorto-ostial coronary artery lesions were excluded from the study. The lesion to scan and treat was selected on operator's discretion after the diagnostic angiogram. NIRS/IVUS and OCT were performed on identical segments of the same coronary artery before PCI. Patients with baseline cTnI levels above ULN were not included in this study. Periprocedural MI was defined as cTnI elevation above 3× ULN measured 6 to 24 h after PCI; patients were divided into 2 groups of cTnI elevation: ≥3× and <3×. Analysis was also performed for the evaluation above 5× ULN in accordance with the third universal definition of MI (22). ULN was defined as 0.5 ng/ml.

Coronary angiographic data and PCI. PCI was performed according to standard methods, and images were stored digitally. About 80% of patients received P2Y$_{12}$ inhibitor loading on the table with maintenance dose for 1 year. All patients received standard bivalirudin bolus and infusion. The target lesion undergoing PCI was identified and quantitative analyses were performed to determine the percentage of diameter stenosis. The lesion to scan and treat was selected based on the operator's discretion after the diagnostic angiogram (1 target lesion per patient). After bivalirudin administration (activated clotting time >300 s), imaging (OCT and combined NIRS-IVUS) was performed. Angiography review was done by a cardiologist (U.B.) who was blinded to patient characteristics and other imaging findings. OCT, IVUS, and NIRS images were analyzed off-line by 3 experienced analysts (Y.V., J.P., S.M.).

OCT image acquisition and analysis. OCT image acquisition was performed with a commercially available C7-XR OCT Intravascular Imaging System (OCT C7 Dragonfly, St. Jude Medical, St. Paul, Minnesota). The OCT catheter was placed at least 10 mm distally to the imaging target lesion. OCT image acquisition was then performed with continuous intracoronary contrast injection (iodixanol) (total volume 12 to 16 ml injected at 3 to 4 ml/s) and simultaneous OCT catheter pullback at 20 mm/s. Each OCT catheter pullback imaged a total of 54 mm of the vessel.

OCT images were analyzed systematically at 1-mm intervals according to previously validated criteria for plaque characterization (23,24) using the St. Jude Medical Offline Review Workstation as we described previously (25,26). The smallest cross-sectional area (CSA), reference CSA, and percentage of lumen area stenosis were calculated for each lesion. For each lipid plaque, the lipid arc was measured at 1-mm intervals through the entire length of the lesion expressed in degrees. Lipid length was measured on longitudinal view (using frame analysis). Lipid

volume index was calculated as the averaged lipid arc multiplied by lipid length (27). Fibrous cap thickness was estimated by measuring the thinnest signal-rich zone separating the lipid content from the vessel lumen in the entire stenosis (in μm). The thinnest part of the fibrous cap was measured 3× and its average was defined as minimum cap thickness. OCT-TCFA was defined as a plaque with lipid arc >90° and fibrous cap thickness <65 μm. Areas with well-defined borders were classified as calcified plaques with the degree of circumferential extent of calcification quantified at 1-mm intervals. Spotty calcification was defined as a calcified plaque <4 mm in length with calcification arc <90° (11). A microchannel was defined as a black hole or tubular structure within a plaque not connected to the vessel lumen and present on at least 3 consecutive cross-sectional OCT images (28). To evaluate the interobserver variability, 3 experienced OCT analysts reviewed OCT pullbacks independently, and the analyses were repeated at intervals of at least 2 weeks by the first observer.

Combined grayscale IVUS and NIRS image acquisition and analysis. Grayscale IVUS and NIRS image acquisition was performed using the commercially available TVC Imaging System with the TVC Insight catheter (Infraredx, Burlington, Massachusetts). Quantitative grayscale IVUS analysis was performed using QIvus 3.0 (MEDIS, Leiden, the Netherlands) to estimate lumen and reference CSA, external elastic membrane CSA, plaque plus media CSA, plaque burden, and remodeling index as described previously (25,26) according to the American College of Cardiology consensus statement (29). Qualitative analysis included ultrasonic attenuation behind the plaque in the absence of calcification (30).

The raw spectra of NIRS estimate the probability of the presence of an atherosclerotic lipid core. The measurements are displayed as a chemogram, which represents a spectroscopic image of the scanned lesion and allows to calculate lipid core burden index (LCBI) (31,32). In the present study, the maximal LCBI was estimated in 4-mm pullback compartments by identifying the maximum LCBI subsegment for every analyzed lesion (maxLCBI$_{4mm}$) as previously described (17).

Image coregistration. OCT and combined NIRS-IVUS pullbacks were coregistered using anatomical landmarks (fiduciary points). Vascular and perivascular markings were used to confirm simultaneous assessment of IVUS measurements and OCT analysis in the same lesion.

Statistical analysis. Interobserver agreement and intraobserver reproducibility of imaging parameter measurements were assessed by intraclass correlation coefficients based on the random effects analysis of variance models (33). The Shapiro-Wilk test was used to assess the normality of continuous data. All continuous measurements were expressed as mean ± SD for normally distributed variables or median and interquartile range (25th percentile, 75th percentile) for nonparametric data and compared using Pearson correlation and Wilcoxon signed-rank test, respectively. Categorical variables are presented as frequencies (percentages) and were compared using the chi-square test or Fisher exact test. To identify the independent correlates of periprocedural MI, we fitted a multivariable logistic regression model with periprocedural MI as the dependent outcome. Variables demonstrating a significant univariable association with this outcome of interest were included as candidate covariates in this model. Given the limited number of outcomes in our study, we performed a sensitivity analysis using both backward and forward stepwise selection to assess model consistency. These analyses yielded similar results to the fully fitted model. The multivariable analyses were performed both for 3× and 5× elevation in cTnI levels for defining MI. Results are reported as unit odds ratios (ORs) with 95% confidence intervals (CIs) and chi-squared. Because OCT imaging emerged as the leading modality for prediction of periprocedural cTnI elevation, another set of analyses was performed by excluding OCT information to critically evaluate the importance of other imaging modalities. All statistical analysis was performed using SPSS statistical software (version 22.0, SPSS Inc., Chicago, Illinois) with a 2-tailed probability value <0.05 considered statistically significant.

RESULTS

Patient characteristics—angiographic and procedural results. The baseline clinical demographics for 110 patients including coronary risk factors and lipid profiles are summarized in Table 1. The mean age of the patients was 63.4 ± 11.9 years, and 83 (75%) were male. cTnI ≥3× ULN was observed in 10 patients (9%); all cTnI ≥3× ULN were male patients (100% vs. 73%, p = 0.06). There were no significant differences in the baseline clinical characteristics between the patients who did or did not develop periprocedural MI. Canadian Cardiovascular Society angina grade III to IV was observed in 63 patients (57%), but there was no difference in severity of angina between the groups (60% vs. 57%, p = 0.85) with and without the troponin leak. Importantly, the number of patients on statins was not different (90% vs. 70%, p = 0.18). The lipid

TABLE 1   Baseline Clinical Demographics

	cTnI Elevation ≥3× (n = 10)	cTnI Elevation <3× (n = 100)	p Value
Age, yrs	59.5 ± 14.0	63.7 ± 11.7	0.29
Male	10 (100)	73 (73)	0.06
Hypertension	8 (80)	91 (91)	0.27
Dyslipidemia	9 (90)	86 (86)	0.73
Diabetes mellitus	5 (50)	40 (40)	0.58
Current smoking	5 (50)	34 (34)	0.31
BMI, kg/m^2	28.3 ± 4.3	29.4 ± 5.9	0.59
Previous MI	0	11 (11)	0.27
CCS angina grade III or IV	6 (60)	57 (57)	0.85
Statin use	9 (90)	70 (70)	0.18
Antiplatelet therapy			0.26
Clopidogrel	7 (70)	85 (85)	
Prasugrel	2 (20)	6 (6)	
Ticagrelor	1 (10)	9 (9)	
GP IIb/IIIa inhibitors	2 (20)	16 (16)	0.74
Total cholesterol, mg/dl	137 (123-155)	141 (119-178)	0.48
HDL cholesterol, mg/dl	38 (32-49)	39 (31-47)	0.87
LDL cholesterol, mg/dl	74 (52-97)	77 (58-110)	0.30
Triglyceride, mg/dl	139 (64-142)	101 (70-146)	0.59

Values are mean ± SD, n (%), or median (interquartile range).

BMI = body mass index; CCS = Canadian Cardiovascular Society; cTnI = cardiac troponin I; GP = glycoprotein; HDL = high-density lipoprotein cholesterol; LDL = low-density lipoprotein cholesterol; MI = myocardial infarction.

profile did not reveal significant differences in total cholesterol (137 vs. 141 mg/dl, p = 0.48), high-density lipoprotein cholesterol (38 vs. 39 mg/dl, p = 0.87), low-density lipoprotein cholesterol (74 vs. 77 mg/dl, p = 0.30), or triglyceride (139 vs. 101 mg/dl, p = 0.59) levels between the cTnI ≥3× and cTnI <3× groups. All patients were treated with antiplatelet therapy; the frequency of each drug was similar in all groups. In

TABLE 2   Angiographic and Procedural Findings

	cTnI Elevation ≥3×	cTnI Elevation <3×	p Value
Target lesion: RCA/LAD/LCX	4/4/2 (40/40/20)	31/53/16 (31/53/16)	0.76
SYNTAX score	8 (3-18)	8 (5-13)	0.91
Degree of stenosis, %	85.5 ± 9.0	83.9 ± 10.0	0.62
Number of treated lesions: 1/2	10/0 (100/0)	94/6 (94/6)	0.43
Number of treated lesions	1 (1-1)	1 (1-1)	0.44
Number of stents: 1/2/3	9/1/0 (90/10/0)	79/19/2 (79/19/2)	0.69
Number of stents	1 (1-1)	1 (1-1)	0.41
Stent length, mm	25 (21-29)	30 (23-38)	0.21
Number of pre-dilations	9 (90)	68 (68)	0.15
Number of post-dilations	7 (70)	78 (78)	0.54
Max balloon pressure, atm	16 (12-16)	16 (14-18)	0.79
Transient no reflow during PCI	3 (30)	0	<0.01

Values are n, median (interquartile range), mean ± SD, or n (%).

LAD = left anterior descending artery; LCX = left circumflex artery; PCI = percutaneous coronary intervention; RCA = right coronary artery; SYNTAX = Synergy Between Percutaneous Coronary Intervention With Taxus and Cardiac Surgery; other abbreviations as in Table 1.

addition, there was no difference in glycoprotein IIb/IIIa Inhibitors use. Of the 10 patients with cTnI ≥3× elevation, 8 patients had ≥5× elevation per recommendation of the third universal definition of MI. Angiographic findings are summarized in Table 2. All lesions were treated with drug-eluting stents. There were no significant differences in the distribution of target lesions, SYNTAX (Synergy Between Percutaneous Coronary Intervention With Taxus and Cardiac Surgery) score, number of treated lesions and implanted stents, stent length, number of pre- and post-dilations, or the maximum balloon pressure. Transient no-reflow was observed in 3 patients from the cTnI ≥3× group (30% vs. 0%, p < 0.01), but post-PCI TIMI (Thrombolysis in Myocardial Infarction) flow grade 3 was achieved in all patients at the end of the procedure and no side branch occlusion was documented.

OCT findings. Pre-PCI OCT findings are shown in Table 3. Although reference lumen CSA was not significantly different between the cTnI ≥3× and cTnI <3× groups, minimum lumen CSA (1.2 vs. 1.9 mm^2, p = 0.02) and lumen area stenosis (80 ± 8% vs. 69 ± 13%, p = 0.03) indicated significantly severe lesions in the cTnI ≥3× group. Maximum lipid arc, lipid length, and lipid volume index were greater in the cTnI ≥3× group. Of 10 cTnI ≥3× patients, 8 (80%) demonstrated ≥180° OCT lipid arc. Minimum cap thickness was significantly lower in the cTnI ≥3× group (55 vs. 90 μm, p < 0.001). Thin fibrous cap (<65 μm) was observed in 29 patients (26%); 9 of 29 (31%) had cTnI ≥3× elevation. Thin fibrous cap was significantly more frequent in the cTnI ≥3× group than in the cTnI <3× group (90% vs. 20%, p < 0.01). TCFA (cap thickness <65 μm and lipid arc >90°) was observed in 27 patients (25%) and was also significantly more frequent in the cTnI ≥3× group (80% vs. 19%, p < 0.01) (Table 3, Figure 1). The thinnest cap was observed proximal to the minimal lumen area (MLA) in 56% and distal to MLA in 19% of TCFA. In 26% of the lesions, the location of the thinnest cap coincided with the minimum lumen site. One TCFA lesion was observed per stenosis. The features of plaque rupture, thrombus, microvessels, and the incidence of spotty calcification were not significantly different between the 2 groups. Intra-class correlation coefficient for interobserver and intraobserver variability for the maximum lipid arc was 0.98 (95% CI: 0.932 to 0.997) and 0.99 (95% CI: 0.965 to 0.998), respectively; for fibrous cap thickness was 0.96 (95% CI: 0.875 to 0.991) and 0.98 (95% CI: 0.933 to 0.997), respectively.

IVUS and NIRS imaging findings. Grayscale IVUS quantitative measurements at the reference location

J A C C : C A R D I O V A S C U L A R I N T E R V E N T I O N S V O L . 8 , N O . 7 , 2 0 1 5
J U N E 2 0 1 5 : 9 3 7 – 4 5

Kini *et al.*   941
Multimodality Imaging for Periprocedural MI

were similar in both groups (Table 3). Minimum lumen CSA was significantly smaller (2.3 ± 0.6 mm² vs. 3.0 ± 0.8 mm², p = 0.02) and the plaque burden was significantly larger (83.8 ± 9.0% vs. 77.1 ± 7.6%, p < 0.01) in the cTnI ≥3× group. Remodeling index tended to be larger in the cTnI ≥3× group (1.10 vs. 0.96, p = 0.06). Our grayscale morphological analysis showed that attenuated plaques were more frequently found in the cTnI ≥3× group (90% vs. 61%, p = 0.02). MaxLCBI$_{4mm}$ was significantly larger in patients with cTnI ≥3× than in those with cTnI <3× (556 vs. 339, p < 0.01). MaxLCBI$_{4mm}$ ≥500 was observed in 33 patients (30%); 8 of 33 (24%) had cTnI ≥3× elevation. MaxLCBI$_{4mm}$ ≥500 was more frequent in the cTnI ≥3× group (80% vs. 25%, p < 0.01). There was an overlap between MLA and maxLCBI$_{4mm}$ segment in the majority of analyzed lesions (85%) in NIRS/IVUS pullback: the maximum lipid segment was proximal to MLA in 11% and distal to MLA in 4% of the lesions.

Predictors of periprocedural MI. With univariate logistic regression analysis, the cap thickness (OR: 0.89, chi-squared: 7.48, p < 0.01) by OCT, plaque burden (OR: 1.16, chi-squared: 6.14, p = 0.01) by IVUS, and maxLCBI$_{4mm}$ (OR: 1.004, chi-squared: 7.18, p < 0.01) by NIRS were important predictors of peri-procedural MI (Table 4). Multivariate logistic regression analysis revealed OCT-verified cap thickness to be the only independent predictor for cTnI≥3× ULN (OR: 0.90, chi-squared: 5.55, p = 0.02); the cap thickness was also the sole predictor of cTnI ≥5× (OR: 0.91, chi-squared: 4.36, p = 0.04). If all OCT findings were excluded from the analysis, plaque burden by IVUS (OR: 1.13, chi-squared: 4.04, p = 0.045) and maxLCBI$_{4mm}$ by NIRS (OR: 1.003, chi-squared: 4.33, p = 0.037) emerged to be the independent predictors. MaxLCBI$_{4mm}$ OR on a per-100-unit LCBI scale is presented in Online Table 1.

DISCUSSION

Although PCI achieves excellent angiographic success, approximately 3% to 15% of cases are complicated by periprocedural MI, which is associated with adverse long-term outcomes (1,2). Whereas numerous studies have previously evaluated the importance of individual imaging findings by OCT, IVUS, or NIRS for the evaluation of periprocedural MI (11,12,14,16), we have done the following: 1) performed head-to-head comparison of the all 3 imaging modalities; 2) demonstrated that OCT-verified TCFA was the only independent predictor for periprocedural MI; and 3) showed that in the absence of information about fibrous cap thickness (or OCT findings), plaque
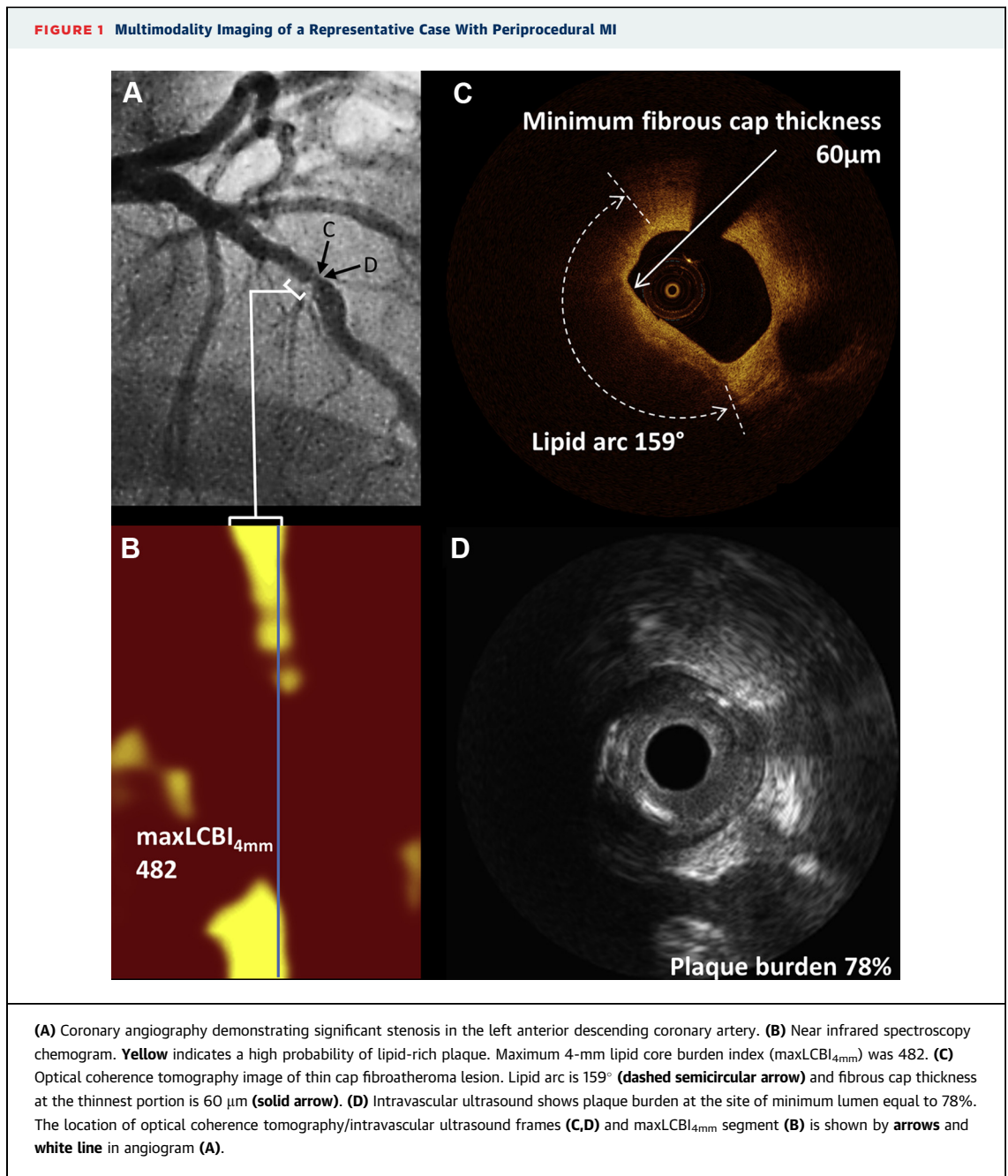
TABLE 3	OCT, IVUS, and NIRS Findings		
	cTnI Elevation ≥3×	cTnI Elevation <3×	p Value
OCT			
Reference lumen CSA, mm²	6.5 (4.0–8.1)	6.4 (4.8–8.1)	0.83
Minimum lumen CSA, mm²	1.2 (1.1–1.3)	1.9 (1.2–2.7)	0.02
Area stenosis, %	79.4 ± 7.8	68.8 ± 13.3	0.03
Lipid arc maximum, °	237 (181–259)	176 (103–265)	0.19
Lipid arc, number of quadrants			0.06
1	1 (10)	21 (21)	
2	1 (10)	30 (30)	
3	7 (70)	28 (28)	
4	1 (10)	21 (21)	
Lipid length, mm	8 (5–11)	5 (2–10)	0.14
Lipid volume index	1,375 (594–2,831)	632 (201–1,431)	0.06
Minimum cap thickness, μm	55 (50–60)	90 (70–120)	<0.01
Minimum cap thickness <65 μm	9 (90)	20 (20)	<0.01
TCFA	8 (80)	19 (19)	<0.01
Plaque rupture	2 (20)	8 (8)	0.21
Thrombus	1 (10)	3 (3)	0.26
Microvessel	4 (40)	46 (46)	0.72
Calcium deposition	10 (100)	78 (78)	0.10
Spotty calcification	7 (70)	41 (41)	0.08
Calcium arc maximum, °	104 (74–265)	107 (75–167)	0.69
IVUS			
Reference			
EEM CSA, mm²	14.6 (9.4–19.1)	13.5 (11.0–16.2)	1.00
Lumen CSA, mm²	8.8 (4.9–11.6)	7.2 (6.0–9.3)	0.70
P&M CSA, mm²	5.1 (2.8–10.1)	5.8 (4.1–7.3)	0.62
Plaque burden, %	40.8 ± 14.0	42.7 ± 12.5	0.66
Minimum lumen site			
EEM CSA, mm²	14.7 (9.7–21.1)	13.1 (10.5–16.0)	0.39
Lumen CSA, mm²	2.3 ± 0.6	3.0 ± 0.8	0.02
P&M CSA, mm²	13.4 (7.6–21.4)	10.6 (8.7–13.8)	0.31
Plaque burden, %	83.8 ± 9.0	77.1 ± 7.6	<0.01
Remodeling index	1.10 (0.97–1.19)	0.96 (0.84–1.10)	0.06
Attenuation	9 (90)	61 (61)	0.02
NIRS			
maxLCBI$_{4mm}$	556 (479–650)	339 (199–512)	<0.01
maxLCBI$_{4mm}$ ≥500	8 (80)	25 (25)	<0.01

Values are median (interquartile range), mean ± SD, or n (%).

CSA = cross-sectional area; cTnI = cardiac troponin I; EEM = external elastic membrane; IVUS = intravascular ultrasound; maxLCBI$_{4mm}$ = maximum 4-mm lipid core burden index; NIRS = near infrared spectroscopy; OCT = optical coherence tomography; P&M = plaque plus media; TCFA = thin cap fibroatheroma.

burden by IVUS or lipid core by NIRS best determined the likelihood of the periprocedural event.

IVUS is a useful tool to measure the lumen and plaque size. However, the spatial resolution of IVUS (approximately 100 to 250 μm) does not allow assessment of cap thickness, and it is difficult to demonstrate lipid area or lipid volume quantitatively. In addition to grayscale IVUS, radiofrequency IVUS or integrated backscatter IVUS facilitate analysis of the plaque composition. Several IVUS studies including a meta-analysis have reported the association of large plaque burden and the extent of necrotic core with

FIGURE 1   Multimodality Imaging of a Representative Case With Periprocedural MI

(A) Coronary angiography demonstrating significant stenosis in the left anterior descending coronary artery. **(B)** Near infrared spectroscopy chemogram. **Yellow** indicates a high probability of lipid-rich plaque. Maximum 4-mm lipid core burden index (maxLCBI$_{4mm}$) was 482. **(C)** Optical coherence tomography image of thin cap fibroatheroma lesion. Lipid arc is 159° **(dashed semicircular arrow)** and fibrous cap thickness at the thinnest portion is 60 μm **(solid arrow)**. **(D)** Intravascular ultrasound shows plaque burden at the site of minimum lumen equal to 78%. The location of optical coherence tomography/intravascular ultrasound frames **(C,D)** and maxLCBI$_{4mm}$ segment **(B)** is shown by **arrows** and **white line** in angiogram **(A)**.

cardiac troponin elevation after PCI (3,15,27). Although this imaging modality has greatly enhanced our understanding of plaque dynamics, it has major limitations. Over the last few years, other imaging techniques with great promise have been employed to provide more insight into plaque composition.

NIRS provides an assessment of the lipid content of plaques by identifying the presence of cholesterol monohydrate and cholesterol ester. Several studies have shown that it can accurately identify lipid-rich regions (26,31,32). We recently demonstrated in the randomized prospective YELLOW (Reduction in Yellow Plaque by Aggressive Lipid Lowering Therapy) trial (34) that short-term intensive statin therapy may reduce lipid content in obstructive lesion as assessed by NIRS. Goldstein et al. (17) described the relationship between the presence of a large lipid core plaque as detected by NIRS and periprocedural MI. Stable patients undergoing PCI were identified from the COLOR registry, a prospective observational study of

patients undergoing NIRS prior to PCI, whereas a large lipid core plaque (maxLCBI$_{4mm}$ >500) was identified in 22.6% of patients, and periprocedural MI only occurred in 9 cases. Importantly, periprocedural MI occurred in 2 cases with maxLCBI$_{4mm}$ <500 as well. NIRS, also, is unable to provide detailed information regarding luminal morphology, dimensions, and plaque composition.

OCT imaging with higher spatial resolution (10 to 20 μm) is able to provide a comprehensive assessment of plaque characteristics such as the presence of macrophages, microchannels, microcalcifications, and the presence of the thin fibrous cap. However, it is difficult to visualize the external elastic membrane contour because of the lower penetration depth (1 to 2 mm) compared with IVUS (4 to 8 mm). The OCT studies to predict periprocedural MI have found the cap thickness and lipid arc to be the predictors of periprocedural MI (13,14,29). It is conceivable that all modalities have distinct strengths, and we compared the relative merits of these imaging techniques in predicting periprocedural injury.

In the present study, the fibrous cap thickness by OCT (OR: 0.90, chi-squared: 5.55, p = 0.02) showed the highest probability to predict periprocedural MI. Because all the target lesions are significantly stenotic, it is conceivable that the thin fibrous cap indirectly indicates the presence of large necrotic or lipid core and the independent demonstration of lipid predominance may not be necessary. In the recursive partition analysis of 295 autopsy specimens from the victims of acute myocardial infarction and sudden death, we similarly observed that the fibrous cap thickness was the most important determinant of the unstable plaques followed by cross-section vascular area stenosis (35). However, once the fibrous cap thickness was excluded from the analysis for plaque vulnerability in the autopsy specimens, the magnitude of the necrotic core and the extent of inflammation emerged as the important determinants. Similar to the autopsy study, on exclusion of fibrous cap thickness (and other OCT parameters) from analyses in the present study, the plaque burden at the minimal lumen area (as assessed by IVUS) (OR: 1.13, chi-squared: 4.04, p = 0.045) and the maximum lipid-core burden index over the 4 mm of plaque (as assessed by NIRS) (OR: 1.003, chi-squared: 4.33, p = 0.037) best explained the periprocedural troponin leak. It is reasonable, then, to deduce that OCT may offer the best imaging modality for predicting periprocedural MI. If the OCT is not available, a combination of IVUS and NIRS may be the subsequent option. Due to the small number of

TABLE 4 Univariate and Multivariate Logistic Regression Analysis for Predicting Periprocedural MI by OCT, IVUS, and NIRS

	Include All Imaging Modalities									Exclude OCT		
	Univariate			Multivariate						Multivariate		
	cTnI Elevation ≥3× (n = 10; 9%)			cTnI Elevation ≥3× (n = 10; 9%)			cTnI Elevation ≥5× (n = 8; 7%)			cTnI Elevation ≥3× (n = 10; 9%)		
	Unit OR (95% CI)	Chi-Squared	p Value	Unit OR (95% CI)	Chi-Squared	p Value	Unit OR (95% CI)	Chi-Squared	p Value	Unit OR (95% CI)	Chi-Squared	p Value
OCT												
Lipid arc, °	1.004 (0.998–1.012)	1.83	0.17									
Lipid length, mm	1.061 (0.949–1.174)	1.27	0.25									
Cap thickness, μm	0.886 (0.796–0.849)	7.48	<0.01	0.896 (0.799–0.962)	5.55	0.02	0.907 (0.809–0.975)	4.36	0.04			
IVUS												
Plaque burden, %	1.161 (1.043–1.326)	6.14	0.01	1.040 (0.927–1.195)	0.38	0.54	1.118 (0.972–1.338)	1.92	0.17	1.134 (1.014–1.300)	4.04	0.045
Remodeling index, %	1.028 (0.995–1.064)	2.70	0.10									
NIRS												
maxLCBI$_{4mm}$	1.004 (1.001–1.007)	7.18	<0.01	1.001 (0.997–1.005)	0.21	0.65	1.000 (0.995–1.004)	0.03	0.87	1.003 (1.000–1.006)	4.33	0.037

CI = confidence interval; OR = odds ratio; other abbreviations as in Tables 1 and 3.

patients and few events, these findings should be considered hypothesis generating rather than a definitive result and warrant substantiation in larger cohorts. It is important to note that regardless of the imaging modality, the incidence of periprocedural complications was low. This is not surprising and confirms similar observations from the COLOR registry (17) and CANARY (Coronary Assessment by Near-Infrared of Atherosclerotic Rupture-Prone Yellow) trial (36).

After post-PCI cardiac enzyme elevation has been reported to be associated with diffuse atherosclerosis (37) and increased adverse short- and intermediate-term outcomes (4-10), the results from the current study do not favor any change in stent placement strategy. Documentation of NIRS-verified large necrotic core alone as the predictor of periprocedural myocardial injury, however, has not justified employing distal protection device in patients undergoing PCI for stable disease (36). Regardless, the results from our analysis suggest that if high-risk plaques (i.e., those with thin fibrous caps) are demonstrated during imaging, the use of more potent antiplatelet therapy (i.e., prasugrel, ticagrelor, glycoprotein IIb/IIIa inhibitors) and maximal dose of statin (as suggested by ARMYDA [Atorvastatin for Reduction of Myocardial Damage During Angioplasty] (38)) could be considered in order to prevent periprocedural MI.

STUDY LIMITATIONS. The small number of events does not allow development of procedural algorithms or determination of receiver-operating characteristic curves or cutoff values of fibrous cap thickness for the likelihood of periprocedural MI. Furthermore, the relationship between cTnI $\geq 3\times$ ULN or $>5\times$ and clinical outcomes is unknown at this time. In addition, the present study did not include patients with ST-segment elevation MI or with non–ST-segment elevation acute coronary syndromes and elevated baseline creatine kinase-myocardial band levels; thus, our results cannot be directly extrapolated to those higher-risk populations. We did not employ IVUS-virtual histology in evaluation of periprocedural myocardial injury, which could have provided similar/superior results and this constitutes a limitation of the current study.

CONCLUSIONS

Periprocedural MI, defined as cTnI $\geq 3\times$ or $5\times$ULN, is a small but distinct complication of PCI with significant consequences. OCT-based fibrous cap thickness is the most important predictor of this complication. Plaque burden or lipid core becomes a determinant only if the information of the fibrous cap thickness is excluded from the analysis. If high-risk plaques are demonstrated during imaging, more potent antiplatelet therapy (i.e., prasugrel, ticagrelor, glycoprotein IIb/IIIa inhibitors) might be of value in preventing periprocedural MI.

REPRINT REQUESTS AND CORRESPONDENCE: Dr. Annapoorna S. Kini, Mount Sinai Hospital, One Gustave L. Levy Place, Box 1030, New York, New York 10029. E-mail: annapoorna.kini@mountsinai.org.

PERSPECTIVES

WHAT IS KNOWN? Myocardial damage after PCI defined as cardiac troponin elevation has been reported as a procedural complication. Although numerous studies have previously evaluated the importance of individual imaging findings by OCT, IVUS, or NIRS for the evaluation of periprocedural MI, it is unclear which of the imaging tools would best allow prediction of this complication.

WHAT IS NEW? Our head-to-head comparison of all 3 imaging modalities demonstrated that OCT-verified TCFA was the only independent predictor for periprocedural MI. Plaque burden by IVUS or lipid core by NIRS best determined the likelihood of the periprocedural event in the absence of information about fibrous cap thickness.

WHAT IS NEXT? Small number of events in the study did not allow development of procedural algorithms or determination of receiver-operating characteristic curves or cutoff values of fibrous cap thickness for the likelihood of periprocedural MI. In addition, further clinical trials are required to determine newer antiplatelet therapy use if TCFA is identified.

REFERENCES

1. Nallamothu BK, Bates ER. Periprocedural myocardial infarction and mortality: causality versus association. J Am Coll Cardiol 2003;42:1412–4.

2. Lansky AJ, Stone GW. Periprocedural myocardial infarction: prevalence, prognosis, and prevention. Circ Cardiovasc Interv 2010;3:602–10.

3. Jang JS, Jin HY, Seo JS, et al. Meta-analysis of plaque composition by intravascular ultrasound and its relation to distal embolization after percutaneous coronary intervention. Am J Cardiol 2013;111:968–72.

4. Kini A, Kini S, Marmur JD, et al. Incidence and mechanism of creatine kinase-MB enzyme elevation after coronary intervention with different

devices. Catheter Cardiovasc Interv 1999;48: 123–9.

5. Garbarz E, Iung B, Lefevre G, et al. Frequency and prognostic value of cardiac troponin I elevation after coronary stenting. Am J Cardiol 1999; 84:515–8.

6. Fuchs S, Kornowski R, Mehran R, et al. Cardiac troponin I levels and clinical outcomes in patients with acute coronary syndromes: the potential role of early percutaneous revascularization. J Am Coll Cardiol 1999;34:1704–10.

7. Cantor WJ, Newby LK, Christenson RH, et al., for the SYMPHONY and 2nd SYMPHONY Cardiac Markers Substudy Investigators. Prognostic significance of elevated troponin I after percutaneous coronary intervention. J Am Coll Cardiol 2002;39: 1738–44.

8. Fujii K, Carlier SG, Mintz GS, et al. Creatine kinase-MB enzyme elevation and long-term clinical events after successful coronary stenting in lesions with ruptured plaque. Am J Cardiol 2005; 95:355–9.

9. Feldman DN, Kim L, Rene AG, Minutello RM, Bergman G, Wong SC. Prognostic value of cardiac troponin-I or troponin-T elevation following non-emergent percutaneous coronary intervention: a meta-analysis. Catheter Cardiovasc Interv 2011;77: 1020–30.

10. Kini AS, Lee P, Marmur JD, et al. Correlation of postpercutaneous coronary intervention creatine kinase-MB and troponin I elevation in predicting mid-term mortality. Am J Cardiol 2004;93:18–23.

11. Ueda T, Uemura S, Watanabe M, et al. Colocalization of thin-cap fibroatheroma and spotty calcification is a powerful predictor of procedure-related myocardial injury after elective coronary stent implantation. Coron Artery Dis 2014;25: 384–91.

12. Porto I, Di Vito L, Burzotta F, et al. Predictors of periprocedural (type IVa) myocardial infarction, as assessed by frequency-domain optical coherence tomography. Circ Cardiovasc Interv 2012;5: 89–96, S1–6.

13. Tanaka A, Imanishi T, Kitabata H, et al. Lipid-rich plaque and myocardial perfusion after successful stenting in patients with non–ST-segment elevation acute coronary syndrome: an optical coherence tomography study. Eur Heart J 2009; 30:1348–55.

14. Lee T, Kakuta T, Yonetsu T, et al. Assessment of echo-attenuated plaque by optical coherence tomography and its impact on post-procedural creatine kinase-myocardial band elevation in elective stent implantation. J Am Coll Cardiol Intv 2011;4:483–91.

15. Shibuya M, Okamura A, Hao H, et al. Prediction of distal embolization during percutaneous coronary intervention for unstable plaques with gray-scale and integrated backscatter intravascular ultrasound. Catheter Cardiovasc Interv 2013;81: E165–72.

16. Amano H, Wagatsuma K, Yamazaki J, Ikeda T. Virtual histology intravascular ultrasound analysis of attenuated plaque and ulcerated plaque detected by gray scale intravascular ultrasound and the relation between the plaque composition and slow flow/no reflow phenomenon during percutaneous coronary intervention. J Interv Cardiol 2013;26:295–301.

17. Goldstein JA, Maini B, Dixon SR, et al. Detection of lipid-core plaques by intracoronary near-infrared spectroscopy identifies high risk of periprocedural myocardial infarction. Circ Cardiovasc Interv 2011;4:429–37.

18. Raghunathan D, Abdel-Karim AR, Papayannis AC, et al. Relation between the presence and extent of coronary lipid core plaques detected by near-infrared spectroscopy with postpercutaneous coronary intervention myocardial infarction. Am J Cardiol 2011;107:1613–8.

19. Kodama T, Kondo T, Oida A, Fujimoto S, Narula J. Computed tomographic angiography-verified plaque characteristics and slow-flow phenomenon during percutaneous coronary intervention. J Am Coll Cardiol Intv 2012;5:636–43.

20. Uetani T, Amano T, Kunimura A, et al. The association between plaque characterization by CT angiography and post-procedural myocardial infarction in patients with elective stent implantation. J Am Coll Cardiol Img 2010;3:19–28.

21. Claessen BE, Maehara A, Fahy M, Xu K, Stone GW, Mintz GS. Plaque composition by intravascular ultrasound and distal embolization after percutaneous coronary intervention. J Am Coll Cardiol Img 2012;5 Suppl 3:S111–8.

22. Thygesen K, Alpert JS, Jaffe AS, et al. Third universal definition of myocardial infarction. J Am Coll Cardiol 2012;60:1581–98.

23. Tearney GJ, Regar E, Akasaka T, et al. Consensus standards for acquisition, measurement, and reporting of intravascular optical coherence tomography studies: a report from the International Working Group for Intravascular Optical Coherence Tomography Standardization and Validation. J Am Coll Cardiol 2012;59:1058–72.

24. Di Vito L, Yoon JH, Kato K, et al., for the COICO Group. Comprehensive overview of definitions for optical coherence tomography-based plaque and stent analyses. Coron Artery Dis 2014;25:172–85.

25. Dohi T, Maehara A, Moreno PR, et al. The relationship among extent of lipid-rich plaque, lesion characteristics, and plaque progression/regression in patients with coronary artery disease: a serial near-infrared spectroscopy and intravascular ultrasound study. Eur Heart J Cardiovasc Imaging 2015;16:81–7.

26. Roleder T, Kovacic JC, Ali Z, et al. Combined NIRS and IVUS imaging detects vulnerable plaque using a single catheter system: a head-to-head comparison with OCT. EuroIntervention 2014;10:303–11.

27. Kato K, Yonetsu T, Kim SJ, et al. Nonculprit plaques in patients with acute coronary syndromes have more vulnerable features compared with those with non-acute coronary syndromes: a 3-vessel optical coherence tomography study. Circ Cardiovasc Imaging 2012;5:433–40.

28. Kitabata H, Tanaka A, Kubo T, et al. Relation of microchannel structure identified by optical coherence tomography to plaque vulnerability in patients with coronary artery disease. Am J Cardiol 2010;105:1673–8.

29. Mintz GS, Nissen SE, Anderson WD, et al. American College of Cardiology Clinical Expert Consensus Document on Standards for Acquisition, Measurement and Reporting of Intravascular Ultrasound Studies (IVUS): a report of the American College of Cardiology Task Force on Clinical Expert Consensus Documents. J Am Coll Cardiol 2001;37:1478–92.

30. Wu X, Mintz GS, Xu K, et al. The relationship between attenuated plaque identified by intravascular ultrasound and no-reflow after stenting in acute myocardial infarction: the HORIZONS-AMI (Harmonizing Outcomes With Revascularization and Stents in Acute Myocardial Infarction) trial. J Am Coll Cardiol Intv 2011; 4:495–502.

31. Gardner CM, Tan H, Hull EL, et al. Detection of lipid core coronary plaques in autopsy specimens with a novel catheter-based near-infrared spectroscopy system. J Am Coll Cardiol Img 2008;1:638–48.

32. Caplan JD, Waxman S, Nesto RW, Muller JE. Near-infrared spectroscopy for the detection of vulnerable coronary artery plaques. J Am Coll Cardiol 2006;47 Suppl 8:C92–6.

33. Kim SJ, Lee H, Kato K, et al. Reproducibility of in vivo measurements for fibrous cap thickness and lipid arc by OCT. J Am Coll Cardiol Img 2012;5: 1072–4.

34. Kini AS, Baber U, Kovacic JC, et al. Changes in plaque lipid content after short-term intensive versus standard statin therapy: the YELLOW trial (Reduction in Yellow Plaque by Aggressive Lipid-Lowering Therapy). J Am Coll Cardiol 2013;62:21–9.

35. Narula J, Nakano M, Virmani R, et al. Histopathologic characteristics of atherosclerotic coronary disease and implications of the findings for the invasive and noninvasive detection of vulnerable plaques. J Am Coll Cardiol 2013;61:1041–51.

36. Stone GW. CANARY: Evaluation of the relationship between intravascular ultrasound and near infrared spectroscopy lipid parameters with periprocedural myonecrosis wth an integrated randomized trial of distal protection to prevent PCI related myocardial infarction. Paper presented at Transcatheter Cardiovascular Therapeutics (TCT) Conference, September 13, 2014; Washington, DC.

37. Kini A, Marmur JD, Kini S, et al. Creatine kinase-MB elevation after coronary intervention correlates with diffuse atherosclerosis, and low-to-medium level elevation has a benign clinical course: implications for early discharge after coronary intervention. J Am Coll Cardiol 1999;34: 663–71.

38. Pasceri V, Patti G, Nusca A, et al., for the ARMYDA Investigators. Randomized trial of atorvastatin for reduction of myocardial damage during coronary intervention: results from the ARMYDA (Atorvastatin for Reduction of MYocardial Damage during Angioplasty) study. Circulation 2004;110:674–8.

KEY WORDS coronary artery disease, percutaneous coronary intervention, periprocedural myocardial infarction, fibrous cap thickness, intravascular imaging

APPENDIX For a supplemental table, please see the online version of this paper.